

# Early Microstructural and Metabolic Changes following Controlled Cortical Impact Injury in Rat: A Magnetic Resonance Imaging and Spectroscopy Study

Su Xu,<sup>1,3</sup> Jiachen Zhuo,<sup>1,3</sup> Jennifer Racz,<sup>2</sup> Da Shi,<sup>1,3</sup> Steven Roys,<sup>1,3</sup> Gary Fiskum,<sup>2,3</sup> and Rao Gullapalli<sup>1,3</sup>

## Abstract

Understanding tissue alterations at an early stage following traumatic brain injury (TBI) is critical for injury management and limiting severe consequences from secondary injury. We investigated the early microstructural and metabolic profiles using *in vivo* diffusion tensor imaging (DTI) and proton magnetic resonance spectroscopy (<sup>1</sup>H MRS) at 2 and 4 h following a controlled cortical impact injury in the rat brain using a 7.0 Tesla animal MRI system and compared profiles to baseline. Significant decrease in mean diffusivity (MD) and increased fractional anisotropy (FA) was found near the impact site (hippocampus and bilateral thalamus;  $p < 0.05$ ) immediately following TBI, suggesting cytotoxic edema. Although the DTI parameters largely normalized on the contralateral side by 4 h, a large inter-individual variation was observed with a trend towards recovery of MD and FA in the ipsilateral hippocampus and a sustained elevation of FA in the ipsilateral thalamus ( $p < 0.05$ ). Significant reduction in metabolite to total creatine ratios of *N*-acetylaspartate (NAA,  $p = 0.0002$ ), glutamate ( $p = 0.0006$ ), *myo*-inositol (Ins,  $p = 0.04$ ), phosphocholine and glycerophosphocholine (PCh+GPC,  $p = 0.03$ ), and taurine (Tau,  $p = 0.009$ ) were observed ipsilateral to the injury as early as 2 h, while glutamine concentration increased marginally ( $p = 0.07$ ). These metabolic alterations remained sustained over 4 h after TBI. Significant reductions of Ins ( $p = 0.024$ ) and Tau ( $p = 0.013$ ) and marginal reduction of NAA ( $p = 0.06$ ) were also observed on the contralateral side at 4 h after TBI. Overall our findings suggest significant microstructural and metabolic alterations as early as 2 h following injury. The tendency towards normalization at 4 h from the DTI data and no further metabolic changes at 4 h from MRS suggest an optimal temporal window of about 3 h for interventions that might limit secondary damage to the brain. Results indicate that early assessment of TBI patients using DTI and MRS may provide valuable information on the available treatment window to limit secondary brain damage.

**Key words:** controlled cortical impact; diffusion tensor imaging; early changes; MR spectroscopy; traumatic brain injury

## Introduction

**T**RAUMATIC BRAIN INJURY (TBI) is a major cause of death and disability worldwide (Langlois et al., 2006; Maas et al., 2008). TBI occurs when an external mechanical force or pressure force (as in the case of blast injury) traumatically injures the brain. The primary injury is characterized by acute biochemical and cellular changes that contribute to continuing neuronal damage and lead to permanent or temporary impairment of physical, cognitive, emotional, and behavioral functions. The biochemical and cellular changes in neurons and glia after TBI are complex and dynamic. The patho-

physiology typically begins with mechanical trauma to the brain (the primary injury), followed rapidly by increased vascular permeability, altered ionic balance, oxidative stress, excitotoxic damage, inflammation, and mitochondrial dysfunction leading to further cell death and injury (secondary injury) (Hovda et al., 1991; Ishige et al., 1988; Kawamata et al., 1995; Lenzlinger et al., 2001; Morganti-Kossmann et al., 2002; Roberson et al., 2006; Xiong et al., 1997; Yang et al., 1985).

Diffusion tensor imaging (DTI) and proton magnetic resonance spectroscopy (<sup>1</sup>H MRS) have recently emerged as powerful approaches for characterizing the microstructural and metabolic responses after TBI. Studies have shown that

<sup>1</sup>Department of Diagnostic Radiology and Nuclear Medicine, <sup>2</sup>Department of Anesthesiology and the Center for Shock Trauma and Anesthesiology Research (STAR), <sup>3</sup>Core for Translational Research in Imaging @ Maryland (C-TRIM), University of Maryland School of Medicine, Baltimore, Maryland.

diffusion-weighted imaging (DWI) and DTI are highly sensitive to tissue microstructure change and axonal damage associated with TBI (Arfanakis et al., 2002; Bazarian et al., 2007; Huisman et al., 2003; Mac Donald et al., 2007a,b; Mayer et al., 2010; Rutgers et al., 2007). In addition to quantifying the average diffusion coefficient of water in the brain, DTI measurements can determine the preferential direction of water diffusion within axons. This information can be used to generate and visualize both normal and abnormal white matter fiber tracts. DTI parameters include mean diffusivity (MD), which measures the average water diffusion within the brain tissue, and fractional anisotropy (FA), which measures the degree of diffusion anisotropy present within axons. The values of FA range from 0 to 1, with highly organized white matter tracts exhibiting higher anisotropy compared to the rest of the brain tissue because of the directionally restrictive structure of bundled axons. Alterations of MD reflect pathological changes in the brain tissue due to changes in the diffusion characteristics of the intra- and extracellular water compartments, including restricted diffusion and water exchange across permeable boundaries (Gass et al., 2002). Change in the FA is indicative of the structural integrity of the tissue. More specifically, the FA change is due to the disproportional change in the diffusion along the neuronal axons (axial diffusivity,  $\lambda_a$ ) and the diffusion perpendicular to the axons (radial diffusivity,  $\lambda_r$ ). Axial diffusivity is believed to be sensitive to axonal integrity and radial diffusivity reflects myelin integrity (Song et al., 2002, 2003). Previous DTI studies on both humans and animals have shown altered MD (Alsop et al., 1996; Huisman et al., 2003; Liu et al., 1999; Mamere et al., 2009), and FA in white matter regions (Arfanakis et al., 2002; Bazarian et al., 2007; Huisman et al., 2004; Mac Donald et al., 2007a,b; Mayer et al., 2010; Wilde et al., 2006; Wozniak et al., 2007) anywhere from 24 h to several days after injury.

In contrast to the structural information offered by DTI regarding brain integrity after TBI, high-resolution *in vivo* proton magnetic resonance spectroscopy provides complementary information and assesses metabolic irregularities following injury. Several of the metabolites detected by  $^1\text{H}$  MRS are highly sensitive to the pathology that contributes to TBI, including hypoxia or ischemia, bioenergetic dysfunction, and inflammation. A majority of clinical TBI studies have consistently found decreases in the neuronal marker *N*-acetylaspartate (NAA) in the brains of TBI patients (Govind et al., 2010; Govindaraju et al., 2004; Macmillan et al., 2002; Marino et al., 2007; Ross et al., 1998). A decrease in NAA (or NAA to total creatine ratio [NAA/tCr], NAA to choline ratio [NAA/Cho]) has been observed within the first 24 h of injury (Holshouser et al., 1997, 2000; Ross et al., 1998), and can remain depressed as long as 8 days after TBI (Brooks et al., 2000; Condon et al., 1998; Holshouser et al., 2005; Ross and Bluml, 2001). While reports of changes in other cerebral metabolites have been less consistent (Brooks et al., 2000; Cecil et al., 1998; Choe et al., 1995; Friedman et al., 1999; Garnett et al., 2000; Marino et al., 2007; Ross et al., 2001; Shutter et al., 2004; Wild et al., 1999; Yeo et al., 2006; Yoon et al., 2005), a few studies on human TBI have shown that the changes in NAA, lactate (Lac), and choline (Cho) are predictive of neurologic outcome 1–25 days post-injury (Brooks et al., 2000; Friedman, 1998, 1999; Garnett et al., 2000; Ross et al., 1998; Signoretti et al., 2002). However, none of these clinical studies addressed the very early changes following TBI.

MRS studies on animal models of TBI have improved our understanding of the metabolic events underlying the injury process and have supported the interpretation of clinical MRS data. As shown in human TBI studies, the metabolic changes in TBI brain may occur over weeks to months following TBI, and these changes may persist for several years post-injury in humans (Brooks et al., 2000; Friedman 1999; Ross et al., 1998). Previous *in vivo*  $^1\text{H}$  MRS studies in various rat model injuries also indicated a time evolution of TBI (Lescot et al., 2010; Schuhmann et al., 2003; Vagnozzi et al., 2007). Schuhmann and colleagues (2003) showed that tCr, NAA, glutamate (Glu), and Cho concentrations significantly decreased during the first 24 h, and then started to increase at 7 days in a controlled cortical impact (CCI) model. At the same time, Lac increased and reached its peak at 7 days after TBI. In a combined DWI and  $^1\text{H}$  MRS study on a lateral fluid percussion injury model, Lescot and associates (2010) reported low ADC values in the brain, which correlated with decreased NAA/tCr and increased Lac level at 24 h after TBI. However, understanding the microstructural and neurochemical changes at very early stages following injury may help in elucidating molecular pathophysiology and determining the time window available for treatment. Further, previous studies have paid very little attention to changes in the brain tissue far removed from injury, for example, in the contralateral hemisphere.

Experimental models of animal TBI are useful for understanding the cerebral microstructure and metabolic mechanisms of brain cell death and neurologic impairment that occur in the various forms and intensities of human TBI (Dixon et al., 1988; Finnie and Blumbergs, 2002; Gennarelli, 1994; Lighthall et al., 1989; Morales et al., 2005; Park et al., 1999). The CCI rat model of TBI uses a known impact interface and a measurable, controllable impact velocity and cortical compression and translates to a repeatable injury with little variability that can be studied over time (Dixon et al., 1988; Hall et al., 2005; Lighthall et al., 1989; Meaney et al., 1994). The features of this model include constant injury reproduction with cortical contusion and distal axonal injury that exhibit cognitive, memory, and motor deficits mimicking human TBI (Chen et al., 1996; Dixon et al., 1991; Tang et al., 1997). We report here for the first time the acute cerebral microstructural and metabolic changes following CCI starting at 2 h using DTI and  $^1\text{H}$  MRS *in vivo* using a 7.0 Tesla scanner.

## Methods

### CCI TBI model

Adult male Sprague-Dawley rats ( $n=8$ , 250–350 g) were subjected to left parietal controlled cortical impact injury (Robertson et al., 2006). TBI was performed using the controlled cortical impact device (Pittsburgh Precision Instruments, Pittsburgh, PA) as previously described (Dixon et al., 1991). Briefly, after being initially anesthetized with 4% isoflurane, the rat was maintained at 2% isoflurane, and the left parietal bone was exposed via a midline incision after positioning it in a stereotactic frame. A high-speed dental drill (Henry Schein, Melville, NY) was used to perform a left-sided craniotomy that was centered 3.5 mm posterior and 4 mm lateral to bregma. A 5 mm round impactor tip was accelerated to 5 m/sec with a vertical deformation depth of 1.0 mm and impact duration of 50 msec consistent with mild injury. The

bone flap was immediately replaced with dental acrylic and the scalp incision was closed with silk. After the surgery, the animal was allowed to recover for about 1.5 h, after which it was transported to MRI for the 2 and 4 h imaging session. The experimental protocol was approved by the Committee for the Welfare of Laboratory Animals of the University of Maryland.

### In vivo DTI and $^1\text{H}$ MRS

All experiments were performed on a Bruker Biospec 7.0 Tesla 30 cm horizontal bore scanner (Bruker Biospin MRI, Ettlingen, Germany). The scanner is equipped with a BGA12S gradient system capable of producing 400 mT/m pulse gradients in each of the three orthogonal axes and interfaced to a Bruker Paravision 5.0 console. A Bruker four-element  $^1\text{H}$  surface coil array was used as the receiver and a Bruker 72 mm linear-volume coil as the transmitter. The rat was anesthetized in an animal chamber using a gas mixture of  $\text{O}_2$  (1 L/min) and isoflurane (3%; IsoFlo, Abbot Laboratories, North Chicago, IL). The animal was then placed prone in a Bruker animal bed and the RF coil was positioned and fixed over the brain. The animal bed was moved to the center of the magnet. At the rest of the experiment, the animals were under 1–2% isoflurane anesthesia and 1 L/min oxygen administration. A MR compatible small-animal monitoring and gating system (SA Instruments, Stony Brook, New York) was used to monitor the animal respiration rate and body temperature. The animal body temperature was maintained at 36–37°C with warm water circulating through the mouse bed. The total duration of the MR imaging and spectroscopic experiment was approximately 2 h at each time point. The animal was under continuous anesthesia from the start of the 2 h imaging session until the completion of the 4 h imaging session.

A three-slice (axial, mid-sagittal, and coronal) scout using fast low-angle shot magnetic resonance imaging (FLASH) (Frahm et al., 1986; Haase et al., 1986) was obtained to localize the rat brain. A fast shimming procedure (Fastmap) was used to improve the  $B_0$  homogeneity within a region of the object (Gruetter et al., 1993). Both proton density- and  $T_2$ -weighted images were obtained using a 2-D rapid acquisition with relaxation enhancement (RARE) sequence (Hennig et al., 1986) (repetition time/effective echo time ( $\text{TR}/\text{TE}_{\text{eff1}}/\text{TE}_{\text{eff2}}$ ) = 5500/18.9/56.8 msec, echo train length = 4, matrix size = 256 × 256, slice thickness = 1 mm, number of averages = 2) covering the entire brain were acquired in both the coronal plane (field of view [FOV] = 3.0 × 3.0 cm<sup>2</sup>) and the axial (FOV = 3.0 × 3.2 cm<sup>2</sup>) plane for anatomic reference. Diffusion tensor images were acquired with single shot spin-echo echo-planar imaging (EPI) sequence in the coronal plane. Diffusion sensitive gradients were applied in 30 non-collinear directions at  $b = 1000 \text{ s/mm}^2$ . Five additional images at  $b = 0 \text{ s/mm}^2$  were also acquired. The acquisition parameters were FOV of 3.0 × 3.0 cm<sup>2</sup> at a matrix resolution of 128 × 128, TR/TE of 6000/50 msec, slice thickness of 1 mm for a total of 24 slices, and two averages and covered the same area as the coronal structural acquisitions. Each rat was scanned at three time points: before the injury and at 2 and 4 h after TBI.

For  $^1\text{H}$  MRS, adjustments of all first- and second-order shims over the voxel of interest were accomplished with the Fastmap procedure. At a TE of 20 msec, the shimming procedure routinely resulted in line-widths of 7–9 Hz of the single

$^1\text{H}$  metabolite resonance (0.023–0.03 ppm). This allowed for a good separation of the glutamate (2.35 ppm) and glutamine (2.45 ppm) peaks (see Fig. 3). The water signal was suppressed by variable power radiofrequency (RF) pulses with optimized relaxation delays (VAPOR) (Tkáč et al., 1999). Outer volume suppression combined with point-resolved spectroscopy (PRESS) sequence (Price and Arata, 1996) from a 3 × 3 × 3 mm<sup>3</sup> voxel was used for signal acquisition, with TR/TE = 2500/20 msec, spectral bandwidth = 4 kHz, number of data points = 2048, number of averages = 300. The voxel covered the immediate pericontusional zone, all layers of the hippocampus, and the superior thalamic structures. MRS data were acquired immediately following the DTI acquisition at each time point in both the pericontusional and the corresponding contralateral voxels (Fig. 3).

### Data processing

Maps of MD and FA were generated offline using FDT (FMRIB's Diffusion Toolbox, Oxford, United Kingdom). Regions of interest (ROIs) were drawn manually on three contiguous slices using ImageJ v1.38x (Wayne Rasband, National Institutes of Health, Bethesda, MD). Regional measures of MD, FA,  $\lambda_a$  (axial diffusivity,  $\lambda_a = \lambda_1$ ) and  $\lambda_r$  (radial diffusivity,  $\lambda_r = (\lambda_2 + \lambda_3)/2$ ) values were obtained from the corpus callosum (CC) and both the ipsilateral and contralateral side of the injury from the hippocampus (hip\_ips, hip\_con), thalamus (tha\_ips, tha\_con), cortex (cor\_ips, cor\_con), the olfactory (of\_ips, of\_con), and fimbria of the hippocampus (fi\_ips, fi\_con), as illustrated in Figure 1.

$^1\text{H}$  MRS data was fitted using the LC-Model package (Provencher, 2001), and only metabolites with standard deviations (SD) % ≤ 20 were included for further analysis. Comparisons of the DTI and MRS parameters were performed for each region of the two hemispheres (uninjured and injured) and at each time point using one way repeated analysis of variance (ANOVA) followed by paired *t*-tests adjusted for multiple comparisons using Bonferroni correction. Statistical significance was defined as  $p < 0.05$ .

## Results

### DTI and $^1\text{H}$ MRS at 2 hours after injury

The  $T_2$ -weighted MR images demonstrated distinct, but heterogeneous lesion at the location of the injury in the left cortical region of the brain at 2 h following CCI (Fig. 1A,B, yellow lines). Although the parameters for CCI injury induction were the same for all the animals, we observed some variability in the extent of bleeding and edema formation between individual animals (Immonen et al., 2009; McIntosh et al., 1989; Smith et al., 1997). Despite the presence of blood products at the site of the injury, the quality of the DTI images was not compromised, as exemplified by the FA and MD images shown in Figure 1D and E, respectively.

Figure 2 shows the average MD, FA,  $\lambda_a$ , and  $\lambda_r$  values from the 11 ROIs shown in Figure 1. In the ipsilateral side, the most obvious alterations in the DTI parameters were in the cortical region where all four DTI parameters were altered significantly. In this region, the MD ( $p = 0.004$ ),  $\lambda_a$  ( $p = 0.018$ ), and  $\lambda_r$  ( $p = 0.002$ ) were significantly decreased while FA ( $p = 0.002$ ) increased. The ipsilateral hippocampus also underwent significant changes where the MD ( $p = 0.01$ ),  $\lambda_a$  ( $p = 0.02$ ), and  $\lambda_r$

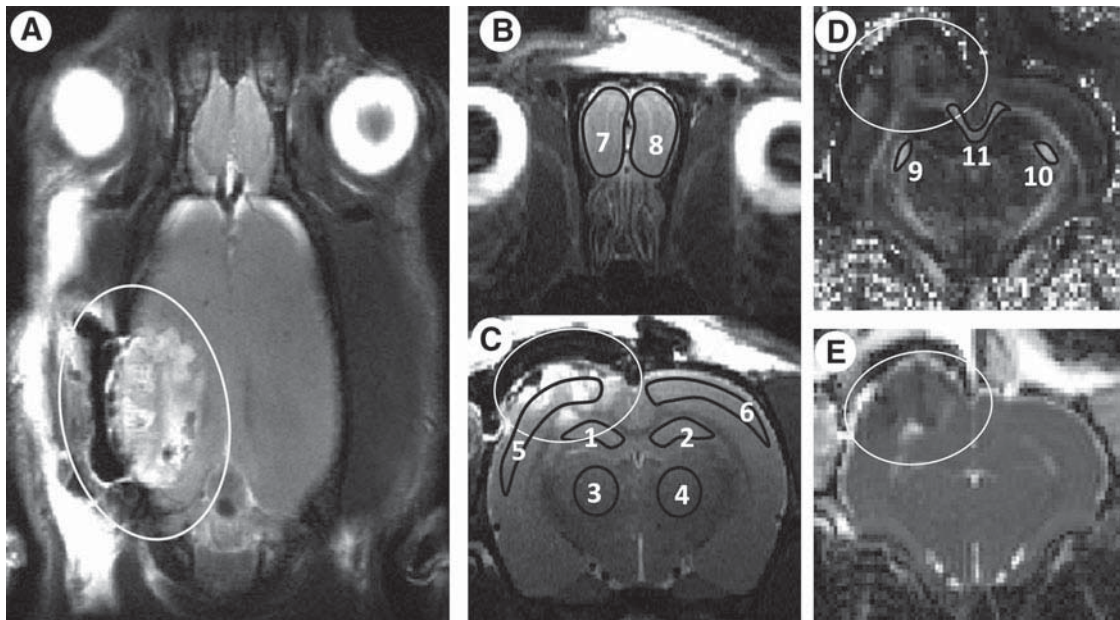


**FIG. 1.** Representative MR images of a rat at 2h after TBI showing the extent of the injury (white contours) and the specific ROIs (black contours). (A) T<sub>2</sub>-weighted axial slice. (B) T<sub>2</sub>-weighted coronal slices showing the placement of the ROIs. (C) Coronal FA and MD maps. ROI 1 and 2, hippocampus; 3 and 4, thalamus; 5 and 6, cortex; 7 and 8, olfactory; 9 and 10, fimbria of hippocampus; 11, corpus callosum.

( $p=0.009$ ) were significantly decreased. A significant increase in FA ( $p=0.003$ ) for the ipsilateral thalamus was observed that was mainly driven by a decrease in  $\lambda_r$  ( $p=0.067$ ). The olfactory region, a remote area from the location of the injury in the cortex, showed a marginal decrease in  $\lambda_a$  ( $p=0.062$ ). It

should be noted that the two white matter-dominated regions, the corpus callosum and fimbria of the hippocampus, which are close to the injury site, showed little alterations in the DTI parameters at 2h following injury. Brain regions contralateral to the injury also experienced significant changes

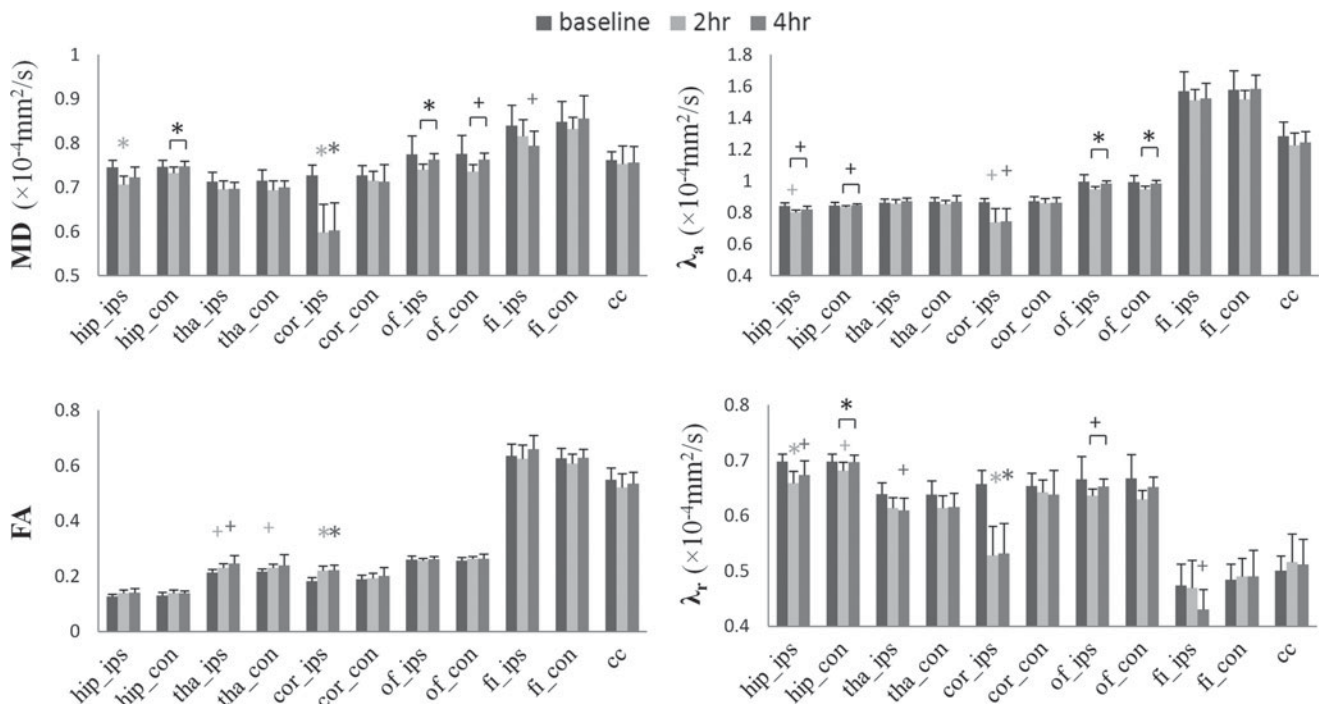


**FIG. 2.** Regional MD, FA,  $\lambda_a$ , and  $\lambda_r$  values at 2 and 4h after TBI for hippocampus ipsilateral (hip\_ips) and contralateral (hip\_con); thalamus ipsilateral (tha\_ips) and contralateral (tha\_con); cortex ipsilateral (cor\_ips) and contralateral (cor\_con); olfactory ipsilateral (of\_ips) and contralateral (of\_con); fimbria of hippocampus ipsilateral (fi\_ips) and contralateral (fi\_con); and corpus callosum (cc). Data are expressed as mean  $\pm$  standard deviation. + $p < 0.05$ ; \* $p < 0.01$ . Cross marks indicate a significant difference between 2 and 4h.

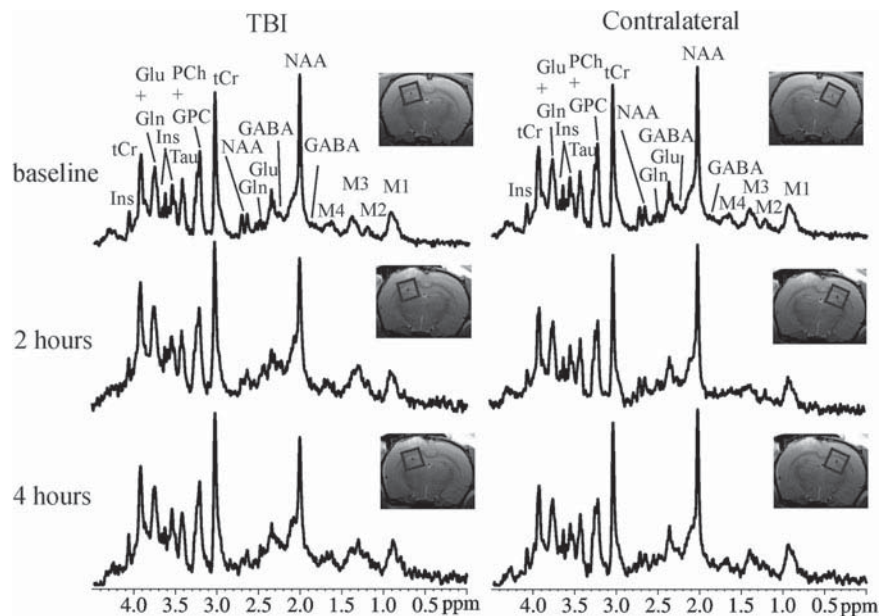


**FIG. 3.** Localized *in vivo*  $^1\text{H}$  spectra and corresponding voxel location depicted on the anatomic image of a TBI rat at 2 and 4 h after injury on both the pericontusional and contralateral sides. GABA,  $\gamma$ -aminobutyric acid; Glu, glutamate; Gln, glutamine; GPC, glycerophosphorylcholine; Lac, lactate; Ins, *myo*-inositol; NAA, *N*-acetylaspartate; PCh, phosphorylcholine; Tau, taurine; +Cr, total creatine. M1, M2, M3 and M4 are macromolecules.

in DTI parameters, including a significant increase in FA in the thalamus ( $p=0.029$ ), marginal decrease in  $\lambda_a$  in the olfactory region ( $p=0.055$ ), and significant decrease in  $\lambda_r$  in the hippocampus ( $p=0.04$ ).

Coronal anatomic images along with the spectroscopic voxel locations in the pericontusional and contralateral region, along with the corresponding spectra from an animal, are shown in Figure 3. The *in vivo*  $^1\text{H}$  spectra demonstrate excellent spectral resolution and sensitivity both at the pericontusional zone and the contralateral sides. At 2 h after injury, the metabolites in the pericontusional zone, including Glu/tCr ( $p=0.0006$ ), PCh+GPC/tCr ( $p=0.03$ ), Ins/tCr ( $p=0.04$ ), NAA/tCr ( $p=0.0002$ ), and Tau/tCr ( $p=0.009$ ) were significantly reduced compared to the baseline, while Gln/tCr was marginally increased ( $p=0.07$ ) (Fig. 4). The contralateral zone also exhibited several biochemical changes after TBI but the changes were milder compared to the pericontusional region (Fig. 5). There was a significant reduction in NAA/tCr (a 6.1% reduction in contralateral zone versus a 29.4% reduction in the pericontusional zone).

#### DTI and $^1\text{H}$ MRS at 4 hours after injury

At 4 h after injury, the DTI parameters near the pericontusional cortical region maintained the same levels as those at 2 h after TBI (Fig. 2). While a marginal recovery of MD ( $p=0.054$ ) and  $\lambda_r$  ( $p=0.07$ ) was seen in the ipsilateral hippocampus in comparison to the 2 h time point, overall these parameters were still reduced compared to the baseline. A further increase in the FA ( $p=0.04$ ) and a reduction in  $\lambda_r$  ( $p=0.02$ ) were observed in the ipsilateral thalamus compared to the baseline. Axial diffusivity,  $\lambda_a$ , which was decreased at the 2 h point normalized to baseline levels in the olfactory region. The DTI parameters for corpus callosum did not undergo any further change compared to the 2 h point. How-

ever, the fimbria of the hippocampus showed significant decrease in both the MD ( $p=0.02$ ) and  $\lambda_r$  ( $p=0.01$ ) compared to the baseline. On the contralateral side, the DTI parameters demonstrated a recovery to the baseline level by 4 h.

Most of the metabolites including Glu/tCr ( $p=0.008$ ), PCh+GPC/tCr ( $p=0.009$ ), Ins/tCr ( $p=0.01$ ), NAA/tCr ( $p=0.0002$ ), and Tau/tCr ( $p=0.0039$ ) continued to be depressed at 4 h following injury compared to the baseline (Fig. 4). In addition, a significant reduction of GABA/tCr ( $p=0.02$ ) was observed by this time compared to the baseline (Fig. 4). The Gln/tCr ratio exhibited more variability compared to the levels observed at 2 h (Fig. 4). Despite these few changes compared to baseline, no significant changes were noted in the ratios of GABA/tCr, Gln/tCr, Glu/tCr, Ins/tCr, NAA/tCr, Tau/tCr, and PCh+GPC/tCr between 2 and 4 h following TBI, which indicates that most significant metabolic alterations occur within 2 h after the injury in the pericontusional zone. In the contralateral side, significant alterations of Ins/tCr ( $p=0.024$ ) and Tau/tCr ( $p=0.013$ ) were observed in the hippocampus. Although, the changes in these metabolites were not as sizeable as in the pericontusional zone, the reductions of Ins/tCr (a 14.8% reduction in contralateral zone versus a 16.6% reduction in the pericontusional zone) and Tau/tCr (a 15.2% reduction in contralateral zone vs. a 12.6% reduction in the pericontusional zone) were statistically significant at 4 h.

#### Discussion

Both experimental and human studies have shown the existence of a temporal window of metabolic vulnerability of TBI (Tavazzi et al., 2007; Vagnozi et al., 2007). However, these experiments were based on repeat concussions on animals, concluding that repeat injuries within 3 days would lead to profound changes in mitochondrial-related mechanism in

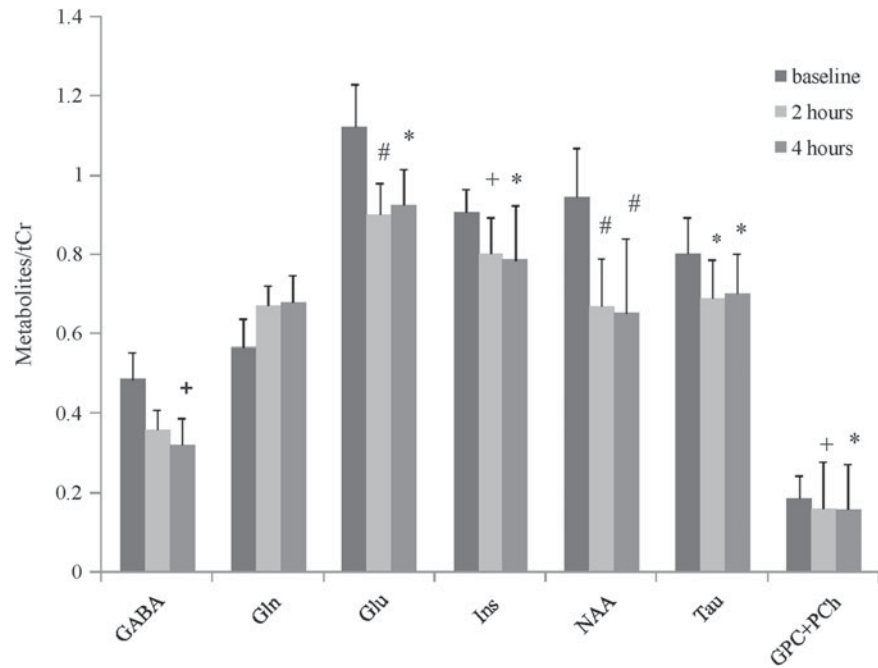


**FIG. 4.** Comparison of the neurometabolic levels in the pericontusional zone before injury (baseline) and at 2 and 4 h after injury in CCI TBI rat brains. Data are expressed as mean  $\pm$  standard deviation. <sup>+</sup> $p < 0.05$ ; <sup>\*</sup> $p < 0.01$ ; <sup>#</sup> $p < 0.001$ .

animal models, which could be easily detected based on reduction in NAA. While these are very important studies to understand the effects of repeat TBIs, we hypothesized that a knowledge of the very early changes in the metabolic profiles and microstructural changes following a single impact injury will have a profound impact on effective management of the injury in the acute stage and lead to the development of neuroprotective agents to reverse or contain the damage from the injury. Because of the sensitivity of DTI and <sup>1</sup>H MRS to

microstructural and metabolic changes *in vivo*, we choose to examine the early changes in the parameters derived from these techniques using a reproducible model of TBI.

We observed decreased MD,  $\lambda_a$  and  $\lambda_r$  and an increased FA as early as 2 h in a variety of regions immediately following TBI, consistent with cytotoxic edema and inflammatory response to the injury. These results agree with the findings from the human TBI studies performed during the acute stage both at the whole brain and regional level (Bazarian et al.,

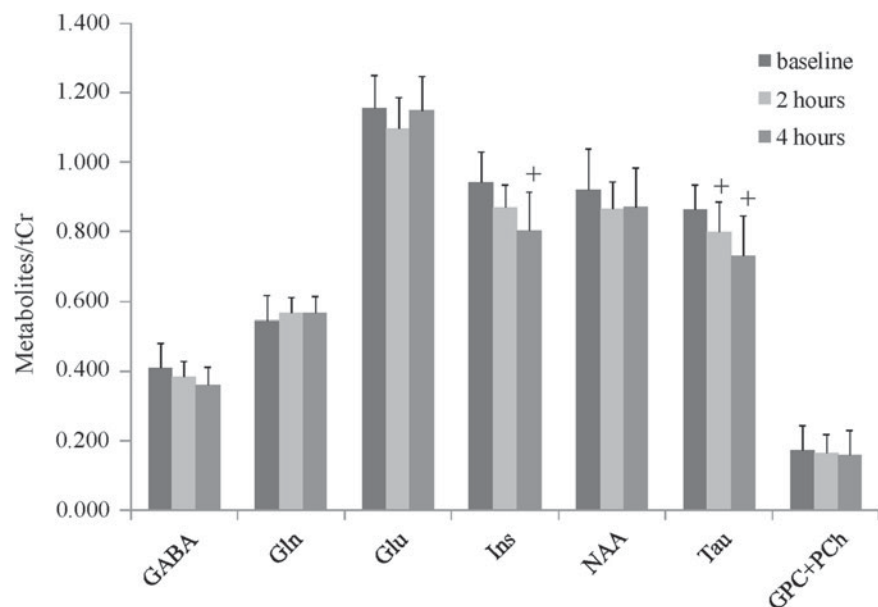


**FIG. 5.** Comparison of the neurometabolic levels in the contralateral zone before injury (baseline) and at 2 and 4 h after injury in CCI TBI rat brain. Data are expressed as mean  $\pm$  standard deviation. <sup>+</sup> $p < 0.05$ ; <sup>\*</sup> $p < 0.01$ ; <sup>#</sup> $p < 0.001$ .

2007; Buki and Povlishock, 2006; Chu et al., 2010; Mayer et al., 2010; Wilde et al., 2008). As expected, ipsilateral cortex was most affected due to direct impact, followed by ipsilateral hippocampus, olfactory, thalamus, and fimbria of the hippocampus. Consistent with the findings from Mac Donald and colleagues (2007a,b), we found that the DTI parameters of the contralateral hippocampus was also altered but to a lesser degree compared to the ipsilateral hippocampus. We also report here for the first time the involvement of the contralateral olfactory cortex and thalamus, suggesting that the injury may lead to disruption in olfaction and executive function (Halbauer et al., 2009; Onyszchuk et al., 2009; Sigurdardottir et al., 2010). In these regions, a decrease in axial diffusivity was accompanied by a stronger decrease in radial diffusivity that contributed to a decrease in MD and an increase in FA. Mayer and colleagues (2010) found increased FA in a prospective study of mild TBI patients in the semi-acute stage and argued that the mechanical forces from TBI result in the stretching of axons and related structures, which alters the function of the gated ion channels, resulting in changes in water homeostasis. Other factors such as high viscosity from cell debris, elevated lipid content within area of necrosis, and decreased water content within myelin sheaths can also limit water diffusivity (Peled, 2007). Taken together, our findings of increased FA and decreases in MD,  $\lambda_a$ , and  $\lambda_r$  suggests reduced extracellular space and highly restricted water diffusion consistent with cytotoxic edema.

<sup>1</sup>H MRS, which covered all layers of the hippocampus and the superior thalamic structures, revealed reductions of Tau/tCr and Ins/tCr. Both Tau and Ins are one of the many organic osmolytes that are regulated in the brain and are believed to be located primarily in glia and absent in the neurons (Brand et al., 1993; Dutton et al., 1991; Lang et al., 1998; Verbalis and Gullans, 1991). Histopathological evidence of astrocyte damage in cortex and hippocampus has been reported in rats as early as 30 min following TBI (Zhao et al., 2003). Current understanding holds that the brain tissue loses a broad range of organic compounds following swelling, including amino acids (Kimmelberg and Mongin, 1998; Law, 1996; Verbalis and Gullans, 1991) and amino acid derivatives, such as Tau and NAA (Olson and Kimmelberg, 1995; Phillis et al., 1998; Sañchez-Olea et al., 1993, 1996; Sager et al., 1997; Taylor et al., 1995). Clinical studies have reported decreased levels of various metabolites, most notably Ins, in a number of patients on whom plasma osmolarity was lowered (Cooper and Wyatt, 2000; HaEussinger et al., 1994; Videen et al., 1995). The reductions of Tau and Ins found in this study may reflect local hyponatremia leading to lowering of intracellular sodium and gain of water, resulting in hypo-osmolality in the vicinity of the impact at the very early stage after injury (Arieff, 1987; Videen et al., 1995). In such situations it has been shown that Ins and Tau are reduced in brain tissue (Bothwell et al., 2001; Silver et al., 2006). It should be noted that in addition to Tau and Ins, NAA, Glu, and GABA are also osmotically active molecules (Bothwell et al., 2001). To date most clinical and experimental animal studies have largely shown an increase in Ins following injury. However the increase in Ins was observed in the sub-acute to chronic stages following TBI and these changes have been attributed to osmolality change due to increased astrocytic activity (Schuhmann et al., 2003; Zhao et al., 2003). Schuhmann and colleagues (2003) observed a decrease of up to 31% for both Ins and Tau during the first 24 h

that eventually rose above the baseline by approximately 31% and 44%, respectively, by 7 days following CCI. Although the early decreases in Ins and Tau were not explained, the authors interpreted the late increase in Ins to be due to increased glial content/glia proliferation. Overall the changes in these metabolites most likely reflect the local tissue osmolality at the very early stages following TBI.

The considerably dynamic decrease in the NAA/tCr during the first 4 h after TBI in this study agrees with the observations from other groups using similar approaches (Schuhmann et al., 2003). We found that the most severe drop of NAA occurred at 2–4 h after the injury in the pericontusional zone. In addition, a much smaller but statistically significant decrease of NAA was observed in the contralateral side, suggesting a global NAA disturbance. Although sharp decrease of NAA immediately after TBI has not yet been fully understood, it may be due to impaired NAA synthesis in the mitochondria (Bates et al., 1996; De Stefano et al., 1995; Lescot et al., 2010; Schuhmann et al., 2003; Signoretti et al., 2008). The nervous system-specific metabolite NAA is synthesized from aspartate and acetyl-coenzyme A, relies on ATP, through the action of L-aspartate N-acetyltransferase in mitochondria or through the cleaving of N-acetyl-aspartyl-glutamate by N-acetylated-a-linked-amino dipeptidase, along with glutamate (Baslow, 2003). Therefore, the synthesis and catabolism of NAA are related to mitochondrial integrity. Our previous mitochondrial respiration study (Robertson et al., 2006) showed mitochondrial dysfunction as early as 1 h after CCI TBI in the pericontusional zone. Several investigations have furnished strong evidence to support the view that initial NAA reduction reflects dysfunctional neurons suffering energetic impairment after TBI (Schuhmann et al., 2003; Signoretti et al., 2001).

The decrease of Glu/tCr in close proximity to the injury at the early stage of CCI agreed with a similar study by Schuhmann and associates (2003). In addition, we found a local reduction of GABA and an accumulation of Gln. At a TE of 20 msec and at a field strength of 7 Tesla, the resonance of Glu (2.35 ppm) and Gln (2.45 ppm) were well resolved, yielding reliable quantification of the metabolites with the coefficient of variation for these metabolites as low as 4–12% for Glu and 8–16% for Gln as reported from LC-Model's processing of spectra. The injury-induced alterations in concentrations of the excitatory neurotransmitter Glu and the inhibitory neurotransmitter GABA may indicate an imbalance in excitatory and inhibitory activity in the hippocampal region at the very early stage of TBI, and therefore may further contribute to the neurological dysfunction caused by TBI. At present, it is thought that the neurotransmission process is completed through the Glu-Gln cycle. The cycle begins with the release of Glu from presynaptic terminals to transport primarily to astrocytes, where it is converted to Gln via the Gln synthetase pathway. The Gln is released back to the neurons, where Glu is regenerated via phosphate-dependent glutaminase, a mitochondrial enzyme. GABA is synthesized by decarboxylation of Glu by glutamic acid decarboxylase. It is possible that the mitochondrial dysfunction caused by the very early stage of TBI may affect the glutaminase activity leading to depletion of Glu, with a compensatory reduction of GABA and an accumulation of Gln. Further studies with electrophysiological correlation may provide more insight into the disruption of the Glu-Gln cycle.

The significant decrease of PCh+GPC/tCr at 4 h after TBI also agrees with other reports (Schuhmann et al., 2003; Viant et al., 2005). As a metabolic marker of myelin and cellular membrane density and integrity (i.e., phospholipid synthesis and degradation), the decrease of PCh+GPC in the initial stage of trauma is possibly a result of membrane degradation in the hippocampus area. Histopathological studies have shown evidence of astrocyte damage in hippocampus in rats as early as 30 min following TBI (Zhao et al., 2003).

The current study did not find a significant increase in the levels of lactate in the mild CCI TBI model. Although, most of the TBI rats did not show significantly elevated Lac levels, one out of the eight rats exhibited a dramatic increase of Lac, coupled with a more severe drop in NAA and Glu although the conventional MRI showed similar levels of injury as that of other rats. While the discrepancy in this one rat is unclear, the presence of Lac has been related to multiple factors, including the increased energy demand to restore the ionic balance (Kawamata et al., 1995) and the disordered mitochondrial dysfunction (Ishige et al., 1988; Unterberg et al., 1988; Yang et al., 1985) at the initial stage of the injury. Future studies with histological verification will need to be performed in order to understand the subtle changes that may be responsible for the ischemic conditions far from the injury, as evidenced from increased lactate from the hippocampus and the thalamic region.

In the current study, the  $^1\text{H}$  MRS data was normalized to the resonance intensity of tCr, as this is present relatively equally in all brain cells and tends to be stable (Arnold and Matthews, 1996). However, Schumann and colleagues (2003) observed a decrease in tCr concentration during the first 24 h under similar experimental conditions as those used in this study. While absolute quantification of tCr was not possible with our data, a reduction in the concentration of tCr would imply that the observed reductions in concentration of various metabolites (except for Gln) are an underestimate and hence the changes are more significant, which does not alter the overall conclusion from this study. Although it is possible that reduction in concentrations of metabolites may be a result of increased creatine, to our knowledge there are no studies that have reported an increase in the concentration of Cr following TBI. Nevertheless, this underscores the importance of monitoring the absolute concentrations of the metabolites for an unbiased estimate. Taken together, these findings of this study indicate that the knowledge of alterations in cerebral metabolites and microstructural changes as early as 2 h post-injury by MRS and DTI, respectively, have the potential to have an impact on the management of TBI patients.

Despite dramatic improvements in the management of TBI, to date there is no effective treatment available to patients, and morbidity and mortality remain high (Hall et al., 2010; Meyer et al., 2010; Stein et al., 2011). At present, there are no FDA-approved pharmacological therapies for acute treatment of TBI patients (Hall et al., 2010). The majority of post-traumatic neurodegeneration is due to secondary pathochemical and pathophysiological cascades that occur during the first few minutes, hours, or days following the injury, which exacerbate the damaging effects of the primary injury. The recently reported clinical trials on acute TBI patients used a 4 h or longer window of treatment (Hall et al., 2010; Stein et al., 2011), which may not be optimum given that we see changes as early as 2 h in the rat model. Although both DTI and MRS

have been studied at the sub-acute and chronic stages among the TBI population, the combined use of these techniques during the early and sub-acute stages has been limited. Early evaluation followed by sub-acute stage evaluation using these techniques may provide insights into the progression of the pathophysiology from the injury that may provide insights into the optimum time window for treatment and also provide the much-needed predictive value in determining outcomes. Given that the combined use of MRS and DTI is sensitive in detecting damage in areas that conventional MRI techniques deem to be normal, they may be very helpful in the early evaluation of patients whose CT and conventional MRI are occult when the clinical status of the patient dictates otherwise. Of particular note is that the DTI and MRS data can complement each other as they assess different aspects of brain parenchyma and appear to be more sensitive compared to the conventional MR imaging techniques used to assess trauma and therefore can be very helpful in the assessment of novel therapeutic strategies (Signoretti et al., 2008; Tollard et al., 2009).

## Conclusion

This study for the first time demonstrates that the combination of information from  $^1\text{H}$  MRS and DTI can detect changes in metabolic and microstructural changes *in vivo* as early as 2 h following CCI in rat brain. The microstructural and neurochemical changes were observed within 2 h following injury in the cortex, hippocampus, and thalamus. In addition, changes in the microstructural environment and neurochemistry extended beyond the site of injury to the contralateral hippocampus and thalamus. The tendency towards normalization of tissue changes as indicated by DTI and no further metabolic changes at 4 h as determined by MRS indicates the existence of a temporal window of about 2 to 3 h for planning interventions that might limit secondary damage to the brain.

## Acknowledgments

This study was supported in part by grants from the National Institutes of Health (1S10RR019935).

## Author Disclosure Statement

No competing financial interests exist.

## References

- Alsop, D.C., Murai, H., Detre, J.A., McIntosh, T.K., and Smith, D.H. (1996). Detection of acute pathologic changes following experimental traumatic brain injury using diffusion-weighted magnetic resonance imaging. *J. Neurotrauma* 13, 515–521.
- Arfanakis, K., Haughton, V.M., Carew, J.D., Rogers, B.P., Dempsey, R.J., and Meyerand, M.E. (2002). Diffusion tensor MR imaging in diffuse axonal injury. *AJNR Am. J. Neuroradiol.* 23, 794–802.
- Arief, A.I. (1987). Hyponatremia associated with permanent brain damage. *Adv. Intern. Med.* 32, 325–344.
- Arnold D.L., and Matthews P.M. (1996). Practical aspects of clinical applications of MRS in the brain, in: *MR Spectroscopy: Clinical Applications and Techniques*. I.R. Young and C.H. Charles (eds). Martin Dunitz: London, pps. 139–159.

- Baslow, M.H. (2003). N-acetylaspartate in the vertebrate brain: metabolism and function. *Neurochem. Res.* 28, 941–953.
- Bates, T.E., Strangward, M., Keelan, J., Davey, G.P., Munro, P.M., and Clark, J.B. (1996). Inhibition of N-acetylaspartate production: implications for  $^1\text{H}$  MRS studies *in vivo*. *Neuroreport* 7, 1397–1400.
- Bazarian, J.J., Zhong, J., Blyth, B., Zhu, T., Kavcic, V., and Peterson, D. (2007). Diffusion tensor imaging detects clinically important axonal damage after mild traumatic brain injury: a pilot study. *J. Neurotrauma* 24, 1447–1459.
- Bothwell, J.H., Rae, C., Dixon, R.M., Styles, P., and Bhakoo, K.K. (2001). Hypo-osmotic swelling-activated release of organic osmolytes in brain slices: implications for brain oedema *in vivo*. *J. Neurochem.* 77, 1632–1640.
- Brand, A., Richterlandsberg, C., and Leibfritz, D. (1993). Multi-nuclear NMR studies on energy-metabolism of glial and neuronal cells. *Dev. Neurosci.* 15, 289–298.
- Brooks, W.M., Stidley, C.A., Petropoulos, H., Jung, R.E., Weers, D.C., Friedman, S.D., Barlow, M.A., Sibbitt, W.L., Jr., and Yeo, R.A. (2000). Metabolic and cognitive response to human traumatic brain injury: a quantitative proton magnetic resonance study. *J. Neurotrauma* 17, 629–640.
- Buki, A., and Povlishock, J.T. (2006). All roads to disconnection? Traumatic axonal injury revisited. *Acta Neurochir.* 148, 181–194.
- Cecil, K.M., Hills, E.C., Sandel, E., Smith, D.H., McIntosh, T.K., Mannon, L.J., Sinson, G.P., Bagley, L.J., Grossman, R.I., Lenkinski, R.E. (1998). Proton magnetic resonance spectroscopy for detection of axonal injury in the splenium of the corpus callosum of brain injured patients. *J. Neurosurg.* 88, 795–801.
- Chen, Y., Constantini, S., Trembovler, V., Weinstock, M., and Shohami, E. (1996). An experimental model of closed head injury in mice: pathophysiology, histology, and cognitive deficits. *J. Neurotrauma* 13, 13557–13568.
- Choe, B.Y., Suh, T.S., Choi, K.Y., Shinn, K.S., Park, C.K., and Kang, J.K. (1995). Neuronal dysfunction in patients with closed head injury evaluated *in vivo*  $^1\text{H}$  magnetic resonance spectroscopy. *Invest. Radiol.* 30, 502–506.
- Chu, Z., Wilde, E.A., Hunter, J.V., McCauley, S.R., Bigler, E.D., Troyanskaya, M., Yallampalli, R., Chia, J.M., and Levin, H.S. (2010). Voxel-based analysis of diffusion tensor imaging in mild traumatic brain injury in adolescents. *AJNR Am. J. Neuroradiol.* 31, 340–346.
- Condon, B., Oluoch-Olunya, D., Hadley, D., Teasdale, G., and Wagstaff, A. (1998). Early  $^1\text{H}$  magnetic resonance spectroscopy of acute head injury: four cases. *J. Neurotrauma* 15, 563–571.
- Cooper, C.E., and Wyatt, J.S. (2000). NMR spectroscopy and imaging of the neonatal brain. *Biochem. Soc. Trans.* 28, 121–126.
- De Stefano, N., Matthews, P.M., and Arnold, D.L. (1995). Reversible decreases in N-acetylaspartate after acute brain injury. *Magn. Reson. Med.* 34, 721–727.
- Dixon, C.E., Lighthall J.W., and Anderson T.E. (1988). Physiologic, histopathologic, and cineradiographic characterization of a new fluid-percussion model of experimental brain injury in the rat. *J. Neurotrauma* 5, 91–104.
- Dixon, C.E., Clifton, G.L., Lighthall, J.W., Yaghmai, A.A., and Hayes, R.L. (1991). A controlled cortical impact model of traumatic brain injury in the rat. *J. Neurosci. Methods* 39, 253–262.
- Dutton, G.R., Barry, M., Simmons, M.L., and Philibert, R.A. (1991). Astrocyte taurine. *Ann. NY Acad. Sci.* 633, 489–500.
- Finnie, J.W., and Blumbergs, P.C. (2002). Traumatic brain injury. *Vet. Pathol.* 39, 679–689.
- Frahm, J., Haase, A., and Matthaei, D. (1986). Rapid NMR imaging of dynamic processes using the FLASH technique. *Magn. Reson. Med.* 3, 321–327.
- Friedman, S.D., Brooks, W.M., Jung, R.E., Chiulli, S.J., Sloan, J.H., Montoya, B.T., Hart, B.L., and Yeo, R.A. (1999). Quantitative proton MRS predicts outcome after traumatic brain injury. *Neurology* 52, 1384–1391.
- Friedman, S.D., Brooks, W.M., Jung, R.E., Hart, B.L., and Yeo, R.A. (1998). Proton MR spectroscopic findings correspond to neuropsychological function in traumatic brain injury. *AJNR Am. J. Neuroradiol.* 19, 1879–1885.
- Garnett, M.R., Blamire, A.M., Corkill, R.G., Cadoux-Hudson, T.A., Rajagopalan, B., and Styles, P. (2000). Early proton magnetic resonance spectroscopy in normal-appearing brain correlates with outcome in patients following traumatic brain injury. *Brain* 123, 2046–2054.
- Gass, A., Niendorf, T., and Hirsch, J.G. (2002). Acute and chronic changes of the apparent diffusion coefficient in neurological disorders—biophysical mechanisms and possible underlying histopathology. *J. Neurol. Sci.* 186, S15–S23.
- Gennarelli, T.A. (1994). Animate models of human head injury. *J. Neurotrauma* 11, 357–368.
- Govind, V., Gold, S., Kaliannan, K., Saigal, G., Falcone, S., Arheart, K.L., Harris, L., Jagid, J., and Maudsley, A.A. (2010). Whole-brain proton MR spectroscopic imaging of mild-to-moderate traumatic brain injury and correlation with neuropsychological deficits. *J. Neurotrauma* 27, 483–496.
- Govindaraju, V., Gauger, G.E., Manley, G.T., Ebel, A., Meeker, M., Maudsley, A.A. (2004). Volumetric proton spectroscopic imaging of mild traumatic brain injury. *AJNR Am. J. Neuroradiol.* 25, 730–737.
- Gruetter, R. (1993). Automatic, localized *in vivo* adjustment of the first- and second-order shim coils. *Magn. Reson. Med.* 29, 804–811.
- Haase, A., Frahm, J., Matthaei, D., Hänicke, W., and Merboldt, K.D. (1986). FLASH imaging: rapid NMR imaging using low flip angle pulses. *J. Magn. Res.* 67, 258–266.
- HaEussinger, D., Laubenberger, J., Vom Dahl, S., Ernst, T., Bayer, S., Langer, M., Gerok, W. and Hennig, J. (1994). Proton magnetic resonance spectroscopy studies on human brain myo-inositol in hypo-osmolarity and hepatic encephalopathy. *Gastroenterology* 107, 1475–1480.
- Halbauer, J.D., Ashford, J.W., Zeitzer, J.M., Adamson, M.M., Lew, H.L., and Yesavage, J.A. (2009). Neuropsychiatric diagnosis and management of chronic sequelae of war-related mild to moderate traumatic brain injury. *J. Rehab. Res. Dev.* 46, 757–796.
- Hall, E.D., Sullivan, P.G., Gibson, T.R., Pavel, K.M., Thompson, B.M., and Scheff, S.W. (2005). Spatial and temporal characteristics of neurodegeneration after controlled cortical impact in mice: more than a focal brain injury. *J. Neurotrauma* 22, 252–265.
- Hall, E.D., Vaishnav, R.A., and Mustafa, A.G. (2010). Antioxidant therapies for traumatic brain injury. *Neurotherapeutics* 7, 51–61.
- Hennig, J., Nauert, A., and Friedburg, H. (1986). RARE-imaging: a fast imaging method for clinical MR. *Magn. Res. Med.* 3, 823–833.
- Holshouser, B.A., Ashwal, S., Luh, G.Y., Shu, S., Kahlon, S., Auld, K.L., Tomasi, L.G., Perkin, R.M., and Hinshaw, D.B., Jr. (1997). Proton MR spectroscopy after acute central nervous system injury: outcome prediction in neonates, infants, and children. *Radiology* 202, 487–496.
- Holshouser, B.A., Ashwal, S., Shu, S., and Hinshaw, D.B., Jr. (2000). Proton MR spectroscopy in children with acute brain

- injury: comparison of short and long echo time acquisitions. *J. Magn. Reson. Imaging* 11, 9–19.
- Holshouser, B.A., Tong, K.A., and Ashwal, S. (2005). Proton MR spectroscopic imaging depicts diffuse axonal injury in children with traumatic brain injury. *AJNR Am. J. Neuroradiol.* 26, 1276–1285.
- Hovda, D.A., Yoshino, A., Kawamata, T., Katayama, Y., and Becker, D.P. (1991). Diffuse prolonged depression of cerebral oxidative metabolism following concussive brain injury in the rat: a cytochrome oxidase histochemistry study. *Brain Res.* 567, 1–10.
- Huisman, T.A., Schwamm, L.H., Schaefer, P.W., Koroshetz, W.J., Shetty-Alva, N., Ozsunar, Y., Wu, O., and Sorensen, A.G. (2004). Diffusion tensor imaging as potential biomarker of white matter injury in diffuse axonal injury. *AJNR Am. J. Neuroradiol.* 25, 370–376.
- Huisman, T.A., Sorensen, A.G., Hergan, K., Gonzalez, R.G., and Schaefer, P.W. (2003). Diffusion-weighted imaging for the evaluation of diffuse axonal injury in closed head injury. *J. Comput. Assist. Tomogr.* 27, 5–11.
- Immonen, R.J., Kharatishvili, I., Niskanen, J.P., Gröhn, H., Pitkänen, A., and Gröhn, O.H. (2009). Distinct MRI pattern in lesional and perilesional area after traumatic brain injury in rat—11 months follow-up. *Exp. Neuro.* 215, 29–40.
- Ishige, N., Pitts, L.H., Berry, I., Nishimura, M.C., and James, T.L. (1988). The effects of hypovolemic hypotension on high-energy phosphate metabolism of traumatized brain in rats. *J. Neurosurg.* 68, 129–136.
- Kawamata, T., Katayama, Y., Hovda, D.A., Yoshino, A., and Becker, D.P. (1995). Lactate accumulation following concussive brain injury: the role of ionic fluxes induced by excitatory amino acids. *Brain Res.* 674, 196–204.
- Kimelberg, H.K., and Mongin, A.A. (1998). Swelling-activated release of excitatory amino acids in the brain: relevance for pathophysiology. *Contr. Nephrol.* 123, 240–257.
- Lang, F., Busch, G.L., and VoEkl, H. (1998). The diversity of volume regulatory mechanisms. *Cell Physiol. Biochem.* 8, 1–45.
- Langlois, J.A., Rutland-Brown, W., and Wald, M.M. (2006). The epidemiology and impact of traumatic brain injury: a brief overview. *J. Head Trauma Rehab.* 21, 375–378.
- Law, R.O. (1996). Volume regulation and the efflux of amino acids from cells in incubated slices of rat cerebral cortex. I. Characteristics of transport mechanisms. *Biochim. Biophys. Acta* 1314, 34–42.
- Lenzlinger, P.M., Morganti-Kossmann, M.C., Laurer, H.L., and McIntosh, T.K. (2001). The duality of the inflammatory response to traumatic brain injury. *Mol. Neurobiol.* 24, 169–181.
- Lescot, T., Fulla-Oller, L., Po, C., Chen, X.R., Puybasset, L., Gillet, B., Plotkine, M., Meric, P., and Marchand-Leroux, C. (2010). Temporal and regional changes after focal traumatic brain injury. *J. Neurotrauma* 27, 85–94.
- Lighthall, J.W., Dixon, C.E., and Anderson, T.E. (1989) Experimental models of brain injury. *J. Neurotrauma* 6, 83–97.
- Liu, A.Y., Maldjian, J.A., Bagley, L.J., Sinson, G.P., and Grossman, R.I. (1999). Traumatic brain injury: diffusion-weighted MR imaging findings. *AJNR Am. J. Neuroradiol.* 20, 1636–1641.
- Maas, A.I., Stocchetti, N., and Bullock, R. (2008). Moderate and severe traumatic brain injury in adults. *Lancet Neurol.* 7, 728–741.
- Mac Donald, C.L., Dikranian, K., Bayly, P., Holtzman, D., and Brody, D. (2007). Diffusion tensor imaging reliably detects experimental traumatic axonal injury and indicates approximate time of injury. *J. Neurosci.* 27, 11869–11876.
- Mac Donald, C.L., Dikranian, K., Song, S.K., Bayly, P.V., Holtzman, D.M., and Brody, D.L. (2007). Detection of traumatic axonal injury with diffusion tensor imaging in a mouse model of traumatic brain injury. *Exp. Neurol.* 205, 116–131.
- Macmillan, C.S., Wild, J.M., Wardlaw, J.M., Andrews, P.J., Marshall, I., and Easton, V.J. (2002). Traumatic brain injury and subarachnoid hemorrhage: *in vivo* occult pathology demonstrated by magnetic resonance spectroscopy may not be ‘ischaemic’. A primary study and review of the literature. *Acta Neurochir.* 144, 853–862.
- Mamere, A.E., Saraiva, L.A., Matos, A.L., Carneiro, A.A., Santos, A.C. (2009). Evaluation of delayed neuronal and axonal damage secondary to moderate and severe traumatic brain injury using quantitative MR imaging techniques. *AJNR Am. J. Neuroradiol.* 30, 947–952.
- Marino, S., Zei, E., Battaglini, M., Vittori, C., Buscalferri, A., Bramanti, P., Federico, A., and De Stefano, N. (2007). Acute metabolic brain changes following traumatic brain injury and their relevance to clinical severity and outcome. *J. Neurol. Neurosurg. Psychiatry* 78, 501–507.
- Mayer, A.R., Ling, J., Mannell, M.V., Gasparovic, C., Phillips, J.P., Doezema, D., Reichard, R., and Yeo, R.A. (2010). A prospective diffusion tensor imaging study in mild traumatic brain injury. *Neurology* 74, 643–650.
- McIntosh, T.K., Vink, R., Noble, L., Yamakami, I., Fernyak, S., Soares, H., and Faden, A.L. (1989). Traumatic brain injury in the rat: characterization of a lateral fluid-percussion model. *Neuroscience* 28, 233–244.
- Meaney, D.F., Ross, D.T., Winkelstein, B.A., Brasko, J., Goldstein, D., Bilston, L.B., Thibault, L.E., and Gennarelli, T.A. (1994). Modification of the cortical impact model to produce axonal injury in the rat cerebral cortex. *J Neurotrauma* 11, 599–612.
- Meyer, M.J., Megyesi, J., Meythaler, J., Murie-Fernandez, M., Aubut, J.A., Foley, N., Salter, K., Bayley, M., Marshall, S., and Teasell, R. (2010). Acute management of acquired brain injury. Part II: an evidence-based review of pharmacological interventions. *Brain Inj.* 24, 706–721.
- Morales, D.M., Marklund, N., Lebold, D., Thompson, H.J., Pitkanen, A., Maxwell, W.L., Longhi, L., Laurer, H., Maegle, M., Neugebauer, E., Graham, D.L., Stocchetti, N., and McIntosh, T.K. (2005). Experimental models of traumatic brain injury: Do we really need to build a better mousetrap? *Neuroscience* 136, 971–989.
- Morganti-Kossmann M.C., Rancan M., Stahel P.F., and Kossmann T. (2002). Inflammatory response in acute traumatic brain injury: a double-edged sword. *Curr. Opin. Crit. Care* 8, 101–105.
- Olson, J.E., and Kimelberg, H.K. (1995). Hypoosmotic volume regulation and osmolyte transport in astrocytes is blocked by an anion transport inhibitor, L-644,711. *Brain Res.* 682, 197–202.
- Onyszczuk, G., Levine, S.M., Brooks, W.M., and Berman, N.E. (2009). Post-acute pathological changes in the thalamus and internal capsule in aged mice following controlled cortical impact injury: a magnetic resonance imaging, iron histochemical, and glial immunohistochemical study. *Neurosci. Lett.* 452, 204–208.
- Park, H.K., Fernandez, I.I., Dujovny, M., and Diaz, F.G. (1999). Experimental animal models of traumatic brain injury: medical and biomechanical mechanism. *Crit. Rev. Neurosurg.* 9, 44–52.
- Peled, S. (2007). New perspectives on the sources of white matter DTI signal. *IEEE Trans. Med. Imaging* 26, 1448–1455.

- Phillis, J.W., Song, D., and O'Regan, M.H. (1998). Tamoxifen, a chloride channel blocker, reduces glutamate and aspartate release from the ischemic cerebral cortex. *Brain Res.* 780, 352–355.
- Price, W.S., and Arata, Y. (1996). The manipulation of water relaxation and water suppression in biological systems using the Water-PRESS pulse sequence. *J. Magn. Reson.* B112, 190–192.
- Provencher, S.W. (2001). Automatic quantitation of localized *in vivo*  $^1\text{H}$  spectra with LCModel. *NMR Biomed.* 14, 260–264.
- Robertson, C.L., Puskas, A., Hoffman, G.E., Murphy, A.Z., Saraswati, M., and Fiskum, G. (2006). Physiologic progesterone reduces mitochondrial dysfunction and hippocampal cell loss after traumatic brain injury in female rats. *Exp. Neurol.* 197, 235–43.
- Ross, B., and Bluml, S. (2001). Magnetic resonance spectroscopy of the human brain. *Anat. Rec.* 265, 54–84.
- Ross, B.D., Ernst, T., Kreis, R., Haseler, L.J., Bayer S., Danielsen, E., Blüml, S., Shonk, T., Mandigo, J.C., Caton, W., Clark, C., Jensen, S.W., Lehman, N.L., Arcinue, E., Pudenz, R., and Shelden, C.H. (1998).  $^1\text{H}$  MRS in acute traumatic brain injury. *J. Magn. Reson. Imaging* 8, 829–840.
- Rutgers, D.R., Toulgoat, F., Cazejust, J., Fillard, P., Lasjaunias, P., and Ducreux, D. (2007). White matter abnormalities in mild traumatic brain injury: a diffusion tensor imaging study. *AJNR Am. J. Neuroradiol.* 29, 51451–51459.
- SaÁnchez-Olea, R., PenÁa, C., MoraÁn, J., and Pasantes-Morales, H. (1993). Inhibition of volume regulation and efflux of osmoregulatory amino acids by blockers of Cl $^-$  transport in cultured astrocytes. *Neurosci. Lett.* 156, 141–144.
- SaÁnchez-Olea, R., Morales, M., GarcÍa, O., and Pasantes-Morales, H. (1996). Cl channel blockers inhibit the volume-activated efflux of Cl and taurine in cultured neurons. *Am. J. Physiol.* 270, C1703–C1708.
- Sager, T.N., Fink-Jensen, A., and Hansen, A.J. (1997). Transient elevation of interstitial *N*-acetylaspartate in reversible global brain ischemia. *J. Neurochem.* 68, 675–682.
- Schuhmann, M.U., Stiller, D., Skardelly, M., Bernarding, J., Klinge, P.M., Samii, A., Samii, M., and Brinker, T. (2003). Metabolic changes in the vicinity of brain contusions: a proton magnetic resonance spectroscopy and histology study. *J. Neurotrauma* 20, 725–743.
- Shutter, L., Tong, K.A., and Holshouser, B.A. (2004). Proton MRS in acute traumatic brain injury: role for glutamate/glutamine and choline for outcome prediction. *J. Neurotrauma* 2, 1693–1705.
- Signoretti, S., Marmarou, A., Aygok, G.A., Fatouros, P.P., Portella, G., and Bullock, R.M. (2008). Assessment of mitochondrial impairment in traumatic brain injury using high-resolution proton magnetic resonance spectroscopy. *J. Neurosurg.* 108, 42–52.
- Signoretti, S., Marmarou, A., Fatouros, P., Hoyle, R., Beaumont, A., Sawauchi, S., Bullock, R., and Young, H. (2002). Application of chemical shift imaging for measurement of NAA in head injured patients. *Acta Neurochir. Suppl.* 81:373–375.
- Signoretti, S., Marmarou, A., Tavazzi, B., Lazzarino, G., Beaumont, A., and Vagnozzi, R. (2001). *N*-Acetylaspartate reduction as a measure of injury severity and mitochondrial dysfunction following diffuse traumatic brain injury. *J. Neurotrauma* 18, 977–991.
- Sigurdardottir, S., Jerstad, T., Andelic, N., Roe, C., and Schanke, A.K. (2010). Olfactory dysfunction, gambling task performance and intracranial lesions after traumatic brain injury. *Neuropsychology* 24, 504–513.
- Silver, S.M., Schroeder, B.M., Sterns, R.H., and Rojiani, A.M. (2006) Myoinositol administration improves survival and reduces myelinolysis after rapid correction of chronic hyponatremia in rats. *J. Neuropathol. Exp. Neurol.* 65, 37–44.
- Smith, D.H., Chen, X.H., Pierce, J.E., Wolf, J.A., Trojanowski, J.Q., Graham, D.I., and McIntosh, T.K. (1997). Progressive atrophy and neuron death for one year following brain trauma in the rat. *J. Neurotrauma* 14, 715–727.
- Song, S.K., Sun, S.W., Ju, W.K., Lin, S.J., Cross, A.H., and Neufeld, A.H. (2003). Diffusion tensor imaging detects and differentiates axon and myelin degeneration in mouse optic nerve after retinal ischemia. *NeuroImage* 20, 1714–1722.
- Song, S.K., Sun, S.W., Ramsbottom, M.J., Chang, C., Russell, J., and Cross, A.H. (2002). Dysmyelination revealed through MRI as increased radial (but unchanged axial) diffusion of water. *NeuroImage* 17, 1429–1436.
- Stein, D.G. (2011). Progesterone in the treatment of acute traumatic brain injury: a clinical perspective and update. *Neuroscience*. 14, [Epub ahead of print].
- Tang, Y.P., Noda, Y., Hasegawa, T., and Nabeshima, T. (1997). A concussive-like brain injury model in mice (II): selective neuronal loss in the cortex and hippocampus. *J. Neurotrauma* 14, 863–873.
- Tavazzi, B., Vagnozzi, R., Signoretti, S., Amorini A.M., Belli, A., Cimatti, M., Delfini, R., Di Pietro, V., Finocchiaro, A., and Lazzarino, G. (2007). Temporal window of metabolic brain vulnerability to concussions: oxidative and nitrosative stresses—part II. *Neurosurgery* 61, 390–395; discussion 395–396.
- Tkác, I., Starcuk, Z., Choi, I.Y., and Gruetter, R. (1999). *In vivo*  $^1\text{H}$  NMR spectroscopy of rat brain at 1 ms echo time. *Magn. Reson. Med.* 41, 649–656.
- Tollard, E., Galanaud, D., Perlberg, V., Sanchez-Pena, P., Le Fur, Y., Abdenmour, L., Cozzone, P., Lehericy, S., Chiras, J., and Pybasset, L. (2009). Experience of diffusion tensor imaging and 1H spectroscopy for outcome prediction in severe traumatic brain injury: preliminary results. *Crit. Care Med.* 37(4), 1448–1455.
- Unterberg, A.W., Andersen, B.J., Clarke, G.D., and Marmarou, A. (1988). Cerebral energy metabolism following fluid-percussion brain injury in cats. *J. Neurosurg.* 68, 594–600.
- Vagnozzi, R., Tavazzi, B., Signoretti, S., Amorini, A.M., Belli, A., Cimatti, M., Delfini, R., Di Pietro, V., Finocchiaro, A., and Lazzarino, G. (2007). Temporal window of metabolic brain vulnerability to concussions: mitochondrial-related impairment—part I. *Neurosurgery* 61, 379–388; discussion 388–389.
- Verbalis, J.G., and Gullans, S.R. (1991). Hyponatremia causes large sustained reductions in brain content of multiple organic osmolytes in rats. *Brain Res.* 567, 274–282.
- Viant, M.R., Lyeth, B.G., Miller, M.G., and Berman, R.F. (2005). An NMR metabolomic investigation of early metabolic disturbances following traumatic brain injury in a mammalian model. *NMR Biomed.* 18, 507–516.
- Videen, J.S., Michaelis, T., Pinto, P., and Ross, B.D. (1995). Human cerebral osmolytes during chronic hyponatremia. *J. Clin. Invest.* 95, 788–793.
- Wild, J.M., Macmillan, C.S.A., Wardlaw, J.M., Marshall, I., Cannon, J., Easton, V.J., and Andrews, P.J.D. (1999).  $^1\text{H}$  spectroscopic imaging of acute head injury—evidence of diffuse axonal injury. *MAGMA* 8, 109–115.
- Wilde, E.A., Chu, Z., Bigler, E.D., Hunter, J.V., Fearing, M.A., Hanten, G., Newsome, M.R., Scheibel, R.S., Li, X., and Levin, H.S. (2006). Diffusion tensor imaging in the corpus callosum in children after moderate to severe traumatic brain injury. *J. Neurotrauma* 23, 1412–1426.

- Wilde, E.A., McCauley, S.R., Hunter, J.V., Bigler, E.D., Chu, Z., Wang, Z.J., Hanten, G.R., Troyanskaya, M., Yallampalli, R., Li, X., Chia, J., and Levin, H.S. (2008). Diffusion tensor imaging of acute mild traumatic brain injury in adolescents. *Neurology* 70, 948–955.
- Wozniak, J.R., Krach, L., Ward, E., Mueller, B.A., Muetzel, R., Schnoebelen, S., Kiragu, A., and Lim, K.O. (2007). Neurocognitive and neuroimaging correlates of pediatric traumatic brain injury: a diffusion tensor imaging (DTI) study. *Arch. Clin. Neuropsychol.* 22, 555–568.
- Xiong, Y., Gu, Q., Peterson, P.L., Muizelaar, J.P., and Lee, C.P. (1997). Mitochondrial dysfunction and calcium perturbation induced by traumatic brain injury. *J. Neurotrauma* 14, 23–34.
- Yang, M.S., DeWitt, D.S., Becker, D.P., and Hayes, R.L. (1985). Regional brain metabolite levels following mild experimental head injury in the cat. *J. Neurosurgery* 63, 617–621.
- Yoon, S.J., Lee, J.H., Kim, S.T., and Chun, M.H. (2005). Evaluation of traumatic brain injured patients in correlation with functional status by localized  $^1\text{H}$ -MR spectroscopy. *Clin. Rehabil.* 19, 209–215.
- Zhao, X., Ahram, A., Berman, R.F., Muizelaar, J.P., Bruce, G., and Lyeth, B.G. (2003). Early loss of astrocytes after experimental traumatic brain injury. *Glia* 44, 140–152.

Address correspondence to:

*Rao Gullapalli, Ph.D.*

*Core for Translational Research in Imaging*

*@ Maryland (C-TRIM)*

*Department of Diagnostic Radiology and Nuclear Medicine*

*University of Maryland School of Medicine*

*22 South Greene Street*

*Baltimore, MD 21201*

*E-mail: gullapalli@umm.edu*